Supporting Information for

Biosensors Based on Acetylcholinesterase Immobilized on Clay-Gold Nanocomposites for the Discrimination of Chlorpyrifos and Carbaryl

Angkana Phongphut[†], Bralee Chayasombat[‡], Anthony E.G. Cass[‖], Muenduen Phisalaphong[†], Seeroong Prichanont[†], Chanchana Thanachayanont[‡], and Thanawee Chodjarusawad[*,§]

[†]Department of Chemical Engineering, Faculty of Engineering, Chulalongkorn University, Phayathai Road, Bangkok 10330, Thailand.

[‡]National Metal and Materials Technology Center, Thailand Science Park, Paholyothin Road, Pathumthani 12120, Thailand.

[§]Department of Physics, Faculty of Science, Burapha University, Long-Hard Bangsaen Road, Chon Buri, 20131, Thailand.

[‖]Department of Chemistry, Imperial College London, London, W12 0NZ, UK

[*] E-mail address: thitikor@buu.ac.th Tel.: (+66) 3810 3143

Figure S1 shows the XPS spectra of Au atom on clay/AuNPs surface that results was tested by X-ray photoelectron spectroscopy (XPS; Kratos AXIS Supra).

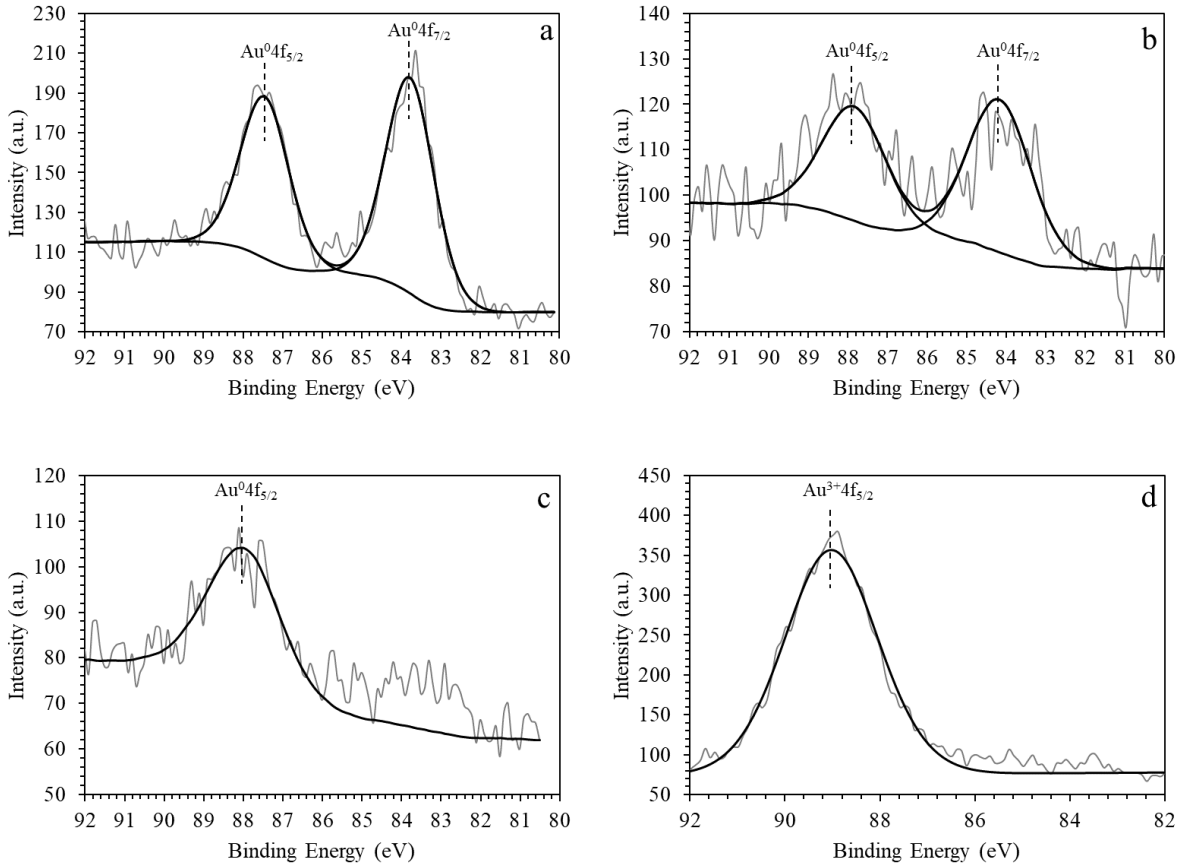

Figure S1. XPS spectra of Au4f at high resolution scan (a) Kaol/AuNPs, (b) Mt/AuNPs, (c) Bent/AuNPs, and (d) Sep/AuNPs.

Figure S2 presents the thermogravimetric analysis (TGA) of clay/AuNPs. The TGA spectra led to the determination of adsorbed water on clay/AuNPs in the region of 100-150°C

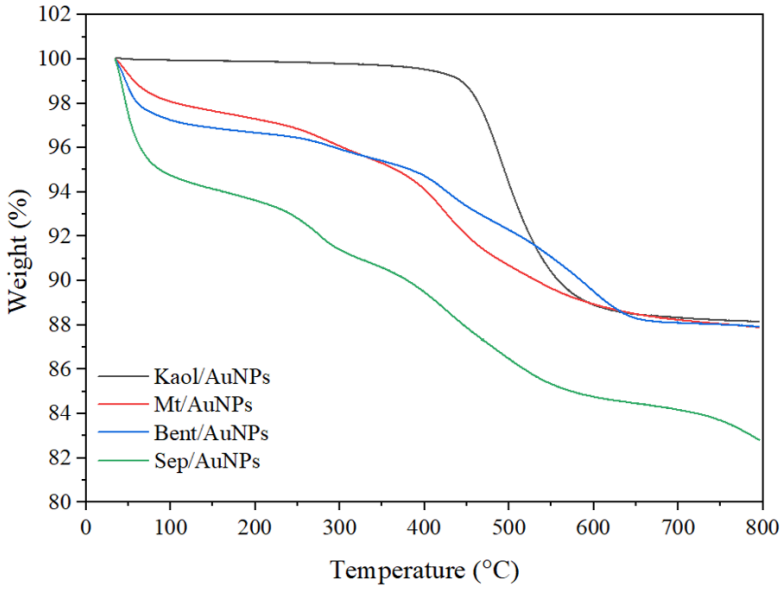

Figure S2. TGA of Kaol/AuNPs (black line), Mt/AuNPs (red line), Bent/AuNPs (blue line), and Sep/AuNPs (green line).

Figure S3 demonstrates the cyclic voltammograms of SPE/clay/CS sensor at different scan rates using our propose sensor as working electrode, commercial Pt and Ag/AgCl electrode as a counter and referent electrode. The results were tested in ferri/ferrocyanide solution and the peak currents were used to calculate the electroactive surface area by Randles–Sevcik equation.

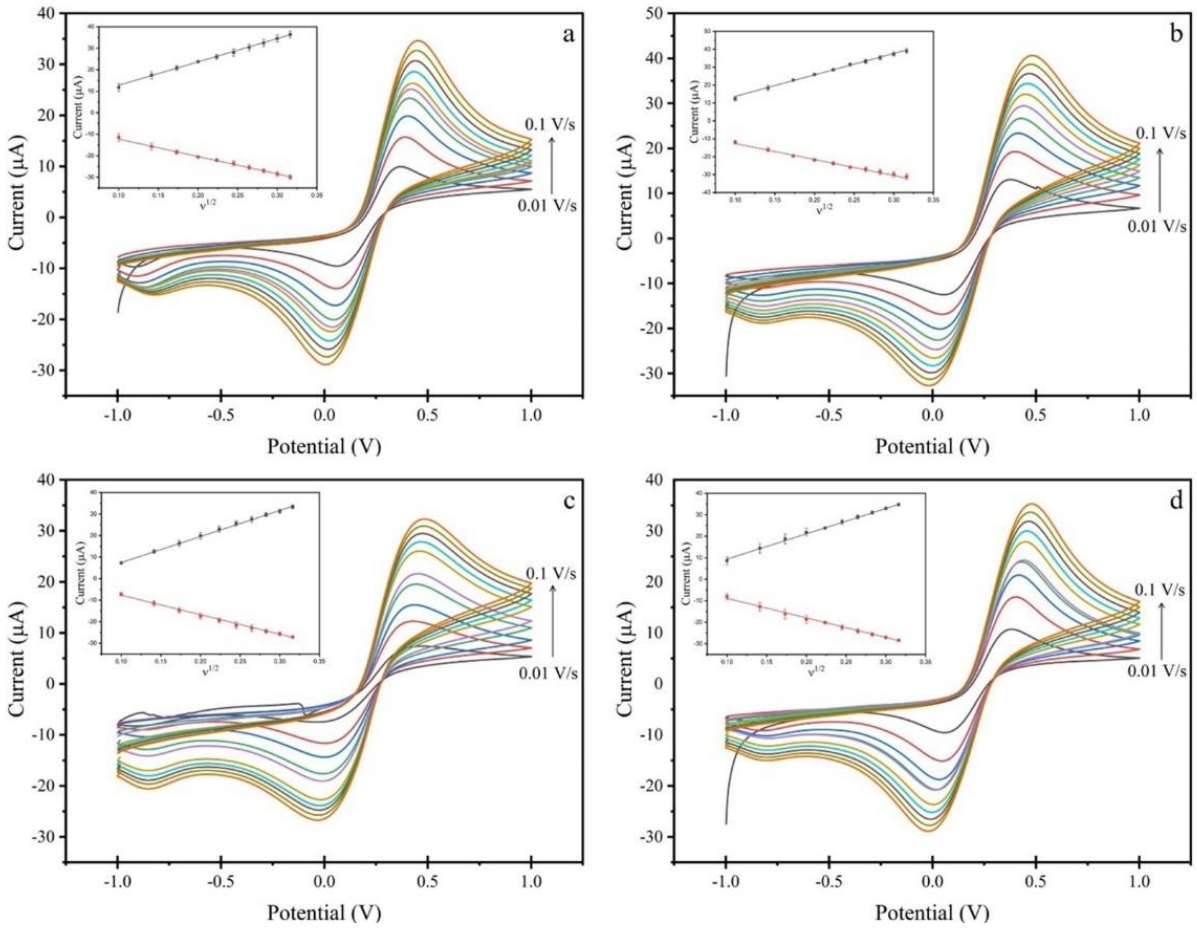

Figure S3 Cyclic voltammograms of (a) SPE/Kaol/CS, (b) SPE/Mt/CS, (c) SPE/Bent/CS, and (d) SPE/Sep/CS at different scan rates in the presence of 10 mM $[Fe(CN)_6]^{3-/4-}$ in 0.1 M PBS (pH 9.0)**.** Insets show plots of the peak current versus square root of the scan rate**.**

Figure S4 shows the cyclic voltammograms of SPE/clay/AuNPs/CS sensor at different scan rates using our propose sensor as working electrode, commercial Pt and Ag/AgCl electrode as a counter and referent electrode. The results were tested in ferri/ferrocyanide solution and the peak currents were used to calculate the electroactive surface area by Randles–Sevcik equation.

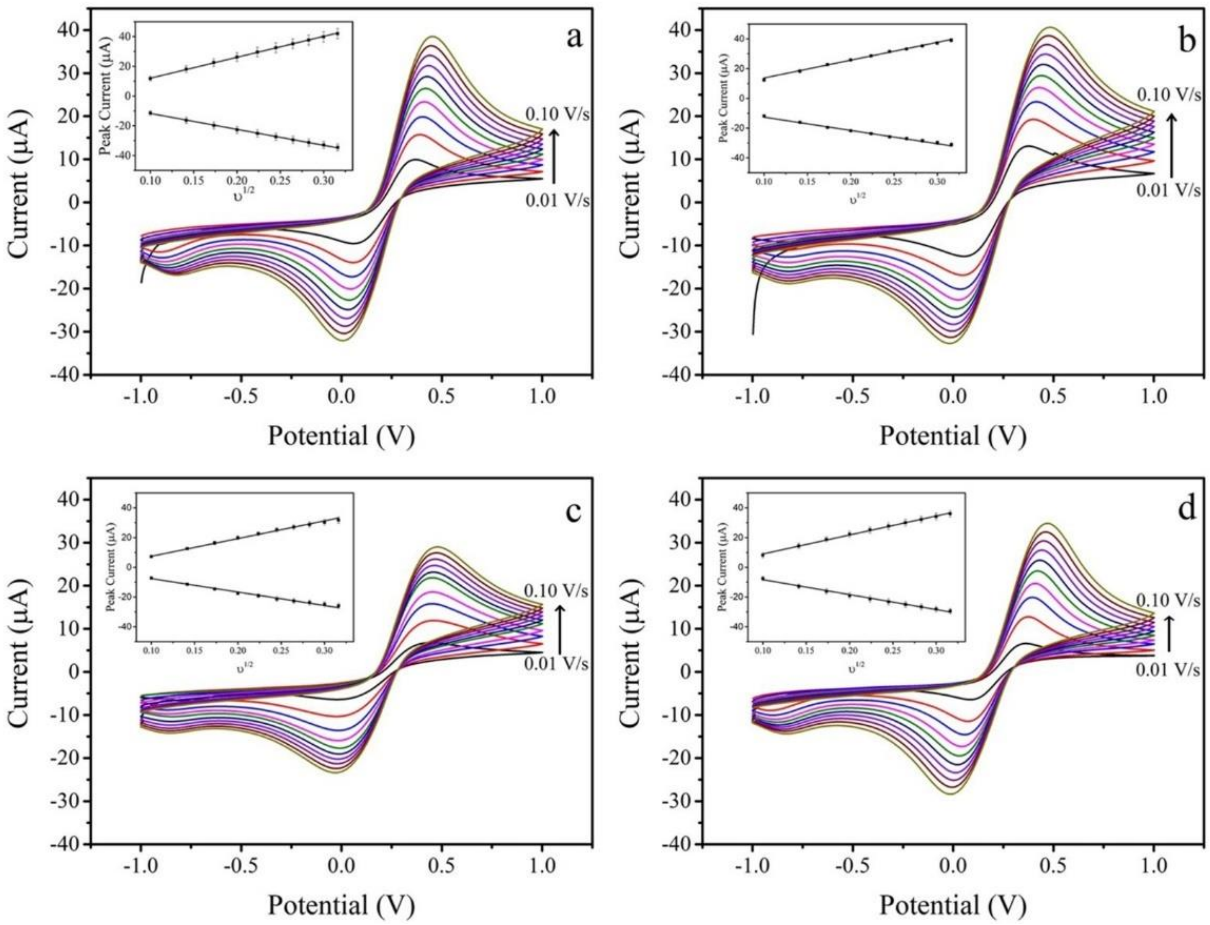

Figure S4. Cyclic voltammograms of (a) SPE/Kaol/AuNPs/CS, (b) SPE/Mt/AuNPs/CS, (c) SPE/Bent/AuNPs/CS, and (d) SPE/Sep/AuNPs/CS at different scan rates in the presence of 10 mM $[Fe(CN)_6]^{3-/4-}$ in 0.1 M PBS (pH 9.0)**.** Insets showplots of the peak current versus square root of the scan rate**.**

Figure S5 shows the cyclic voltammograms of SPE/clay/AuNPs/AChE/CS sensor at different scan rates in acetylthiocholine chloride (ATCh) solution using our propose sensor as working electrode, commercial Pt and Ag/AgCl electrode as a counter and referent electrode. The peak currents are increase with the square root of the scan rates that indicate a diffusion-control process of SPE/clay/AuNPs/AChE/CS.

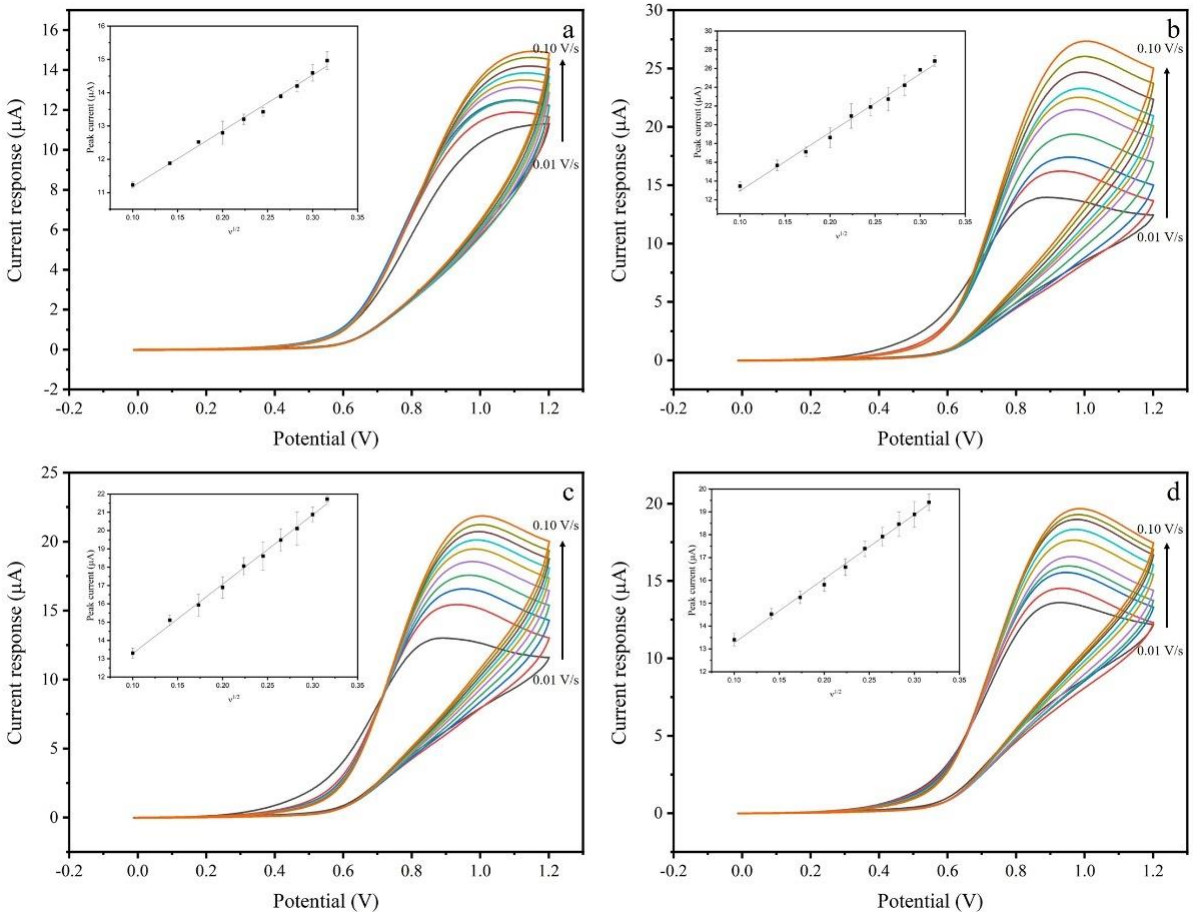

Figure S5. Cyclic voltammograms of (a) SPE/Kaol/AuNPs/AChE/CS, (b) SPE/Mt/AuNPs/AChE /CS, (c) SPE/Bent/AuNPs/AChE /CS, and (d) SPE/Sep/AuNPs/AChE /CS at different scan rates in the presence of 10 mM ATCh in 0.1 M PBS (pH 9.0)**.** Insets showplots of the peak current versus square root of the scan rate**.**

Figure S6 presents the current response of SPE/clay/AuNPs/AChE/CS sensor at different pH solution which was obtained from the amperometric method using our propose sensor as working electrode, commercial Pt and Ag/AgCl electrode as a counter and referent electrode.

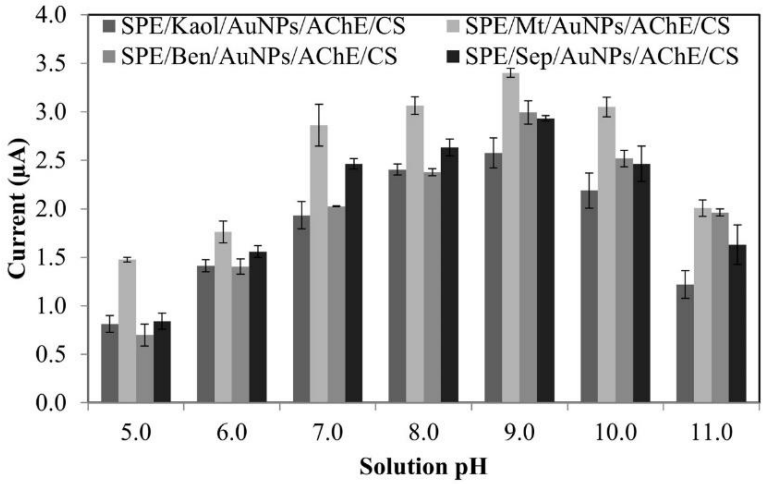

Figure S6. The effect of solution pH on the amperometric current response of clay/AuNPs/AChE/CS biosensors in the presence of 10 mM ATCh in 0.1 M PBS (pH 9.0)

Figure S7 presents the current response of SPE/clay/AuNPs/AChE/CS sensor at different substrate concentrations (ATCh). The results were measured by the amperometric method at the oxidation peak potential of each sensor using our propose sensor as working electrode, commercial Pt and Ag/AgCl electrode as a counter and referent electrode.

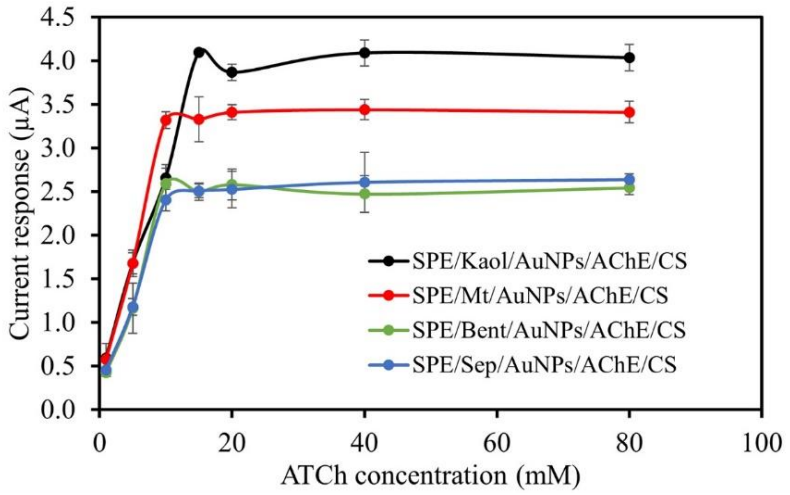

Figure S7. Effect of ATCh concentration (1 - 80 mM) on the current response of SPE/Kaol/AuNPs/AChE/CS, SPE/Mt/AuNPs/AChE/CS, SPE/Bent/AuNPs/AChE/CS, and SPE/Sep/AuNPs/AChE/CS biosensors.

Figure S8 demonstrates the optimum inculbation time of SPE/clay/AuNPs/AChE/CS sensor on chlorpyrifos and carbaryl determination. The results were measured by amperometric method at optimum potential, ATCh concentration and solution pH using our propose sensor as working electrode, commercial Pt and Ag/AgCl electrode as a counter and referent electrode.

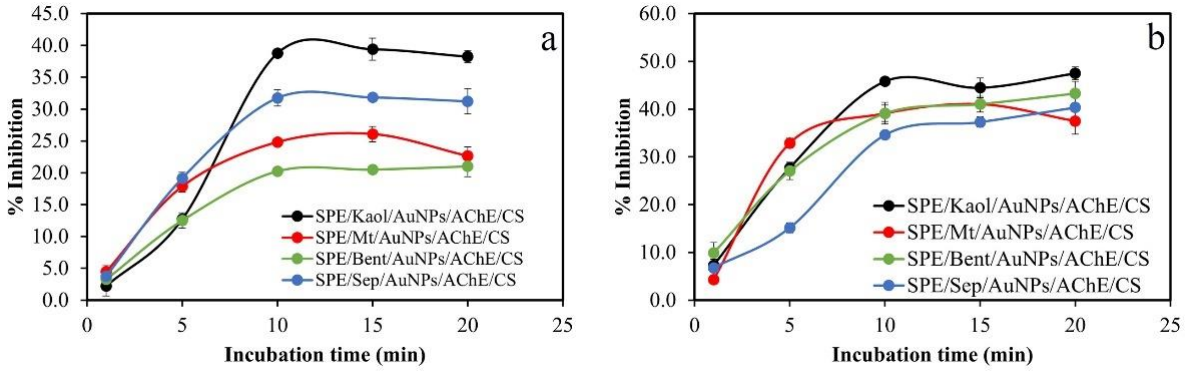

Figure S8. Effect of the incubation time of 200 ng/mL chlorpyrifos (a) and 200 ng/mL carbaryl (b) on the %inhibition of SPE/Kaol/AuNPs/AChE/CS, SPE/Mt/AuNPs/AChE/CS, SPE/Bent/AuNPs/AChE/CS, and SPE/Sep/AuNPs/AChE/CS biosensors.

Figure S9 shows the %inhibition of SPE/clay/AuNPs/AChE/CS sensors at different concentration ratios of the binary mixtures of chlorpyrifos and carbaryl. The results were measured using an amperometric method at the optimum conditions of each biosensor using our modified electrode, commercial Pt, and Ag/AgCl as a working, counter, and reference electrodes, respectively.

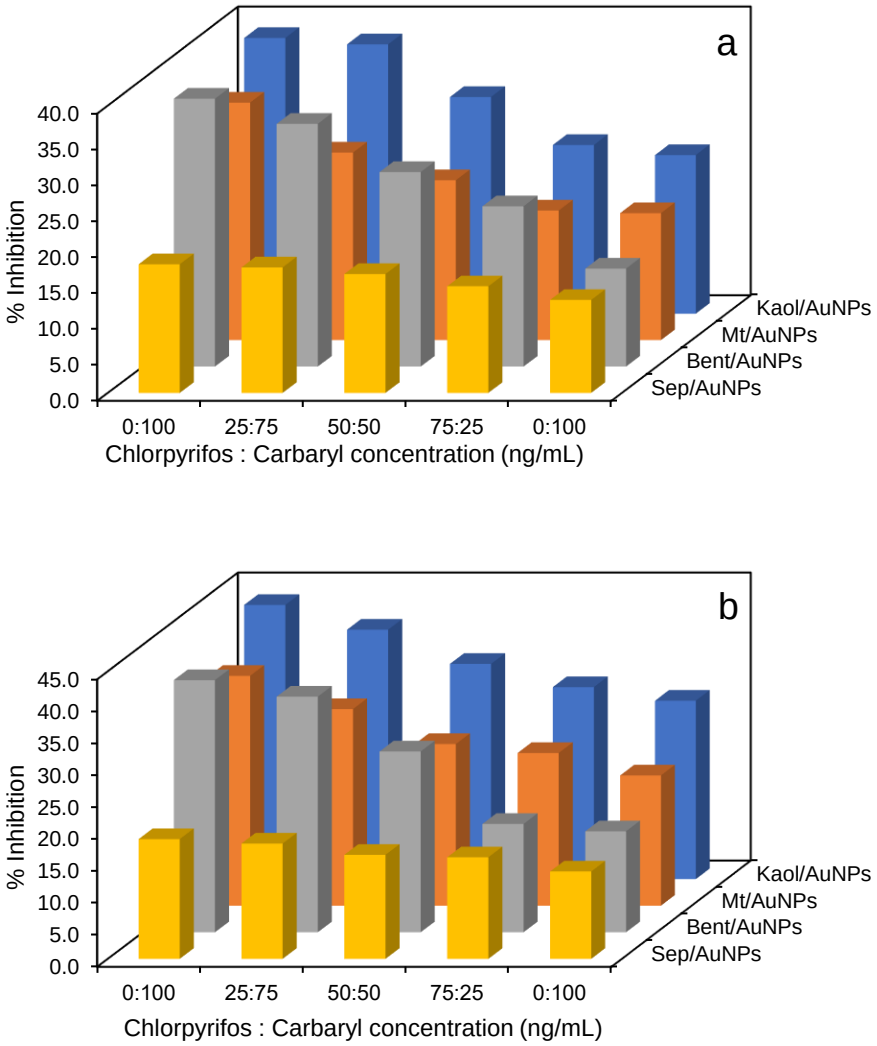

Figure S9. SPE/clay/AuNPs/AChE/CS sensors for determination of chlorpyrifos and carbaryl mixtures at different concentration ratios (a) in synthetic solutions and (b) in carrot samples

Table S1 Current responses of SPE/clay/AuNPs/AChE/CS biosensor

Batch number	Kaol/AuNPs	Mt/AuNPs	Bent/AuNPs	Sep/AuNPs
1	4.40	3.29	2.59	2.70
2	3.98	3.54	2.45	2.57
3	3.83	3.40	2.59	2.64
4	4.09	3.63	2.46	2.35
5	4.10	3.61	2.69	2.94
6	4.09	3.07	2.27	2.47
7	3.97	3.32	2.75	2.35
8	4.19	3.43	2.59	2.47
9	3.96	3.48	2.40	2.76
10	4.06	3.62	2.47	2.44
Average	4.07	3.44	2.53	2.57
SD	0.15	0.18	0.14	0.19
R.S.D. (%)	3.77	5.15	5.67	7.46